

Interpretation of Aeromagnetic Data to Delineate Structural Complexity Zones and Porphyry Intrusions at Samr El Qaa Area, North Eastern Desert, Egypt

Sayed O. Elkhateeb¹, Ahmed M. Eldosouky², Aboelabas Samir¹

¹Department of Geology, Faculty of science, South Valley University, 83523, Qena, Egypt, ²Egyptian Environmental Affairs Agency (E.E.A.A.), Egypt

Corresponding Author: ¹Ahmed Mohammed Eldosouky. Researcher at National Conservation Sector, Egyptian Environmental Affairs Agency, Egypt

Author Email: ahmed.dswky@sci.svu.edu.eg, dr_a.eldosoky@yahoo.com

Abstract: The present investigation is based on the enhancement of the Reduced to the pole map of Samr El-Qaa area, North Eastern Desert, Egypt to delineate porphyry intrusions and junction zones. Detection of shear zones and porphyry structures from magnetic grids can be successfully used as a primary indication for areas of hydrothermal deposits in regional territories. Center for Exploration Targeting (CET) Grid enhancement was applied to magnetic data of Samr El-Qaa region for producing the map of structural complexity zones. Furthermore, the CET Porphyry technique was utilized to derive the likely near circular features. From the CET maps, it can clearly reveal that the major structural trends are N-S, NNE, NNW, NW and NE directions and the dike-like structures and porphyry intrusions in Samr El-Qaa area are aligned along these extracted trends. CET porphyry map showed the areas that can contain various occurrences of porphyry minerals in Samr El-Qaa area. The predicted positions of porphyry intrusion and junction regions can be used as primary maps for the mineral investigation of Samr El-Qaa territory.

Keywords: Samr El-Qaa, Aeromagnetic, CET, Structural Complexity, Porphyry Intrusions.

1. INTRODUCTION

Magnetic data is considered as one of the most effective suitable tools that promote the identification of the geologic structures. The utilization of the magnetic analysis can be used in mapping regional junction regions, dike-like structures, deep contacts, rock differentiation localities, the depth of the sedimentary cover, and mineralization (Domzalski, 1966).

Magnetic data investigation and enhancement provided mapping the surface and deep geologic frames (Sharma 1997) and revealing junction regions and porphyry intrusion (Holden et al., 2011). These structural characteristics are exhibited in trends and intensities apparent on aeromagnetic data that interpreting magnetic patterns (Gay, 1972).

Moreover, the texture examination allowed improving and distinguishing geologic features like lithologic contacts, faults, and joints (Eldosouky and Elkhateeb, 2017). On the other hand, porphyry zones are associated with the igneous intrusion in nature which appears a near circular-feature. Hydrothermal alteration often surrounded the intrusion revealing subsequent/concentric zones. As the porphyry deposits are considered the world's predominant source of molybdenum,

copper, gold, silver and other by-product metals, the investigations for porphyry intrusions are significance. Magnetic data have the energy to describe the porphyry intrusions and geologic structures (Eldosouky et al., 2017).

Therefore, various investigations focused on identifying the structural characteristics and porphyry intrusions using aeromagnetic data (Holden et al., 2008; Core et al., 2009; Williams and Shah 1990; Eldosouky et al., 2017).

Samr El-Qaa territory was examined by many researchers. Said (1962) and El-Gaby (1983) explained the structural and tectonic framework of the study district. Bayoumi and Boctor (1970) and Abdel-Rahman and El-Etr (1980) employed electromagnetic, magnetic, and gravity data to recognize the depth to basement and the structures of Samr El-Qaa area.

The purpose of the existing work is to evaluate aeromagnetic data for delineating structural complexity zones and porphyry structures of Samr El-Qaa region using CET grid and porphyry techniques.

2. GEOLOGIC SETTING OF THE STUDY AREA

Samr El-Qaa territory is situated to the west of Ras Gharib Town in the North Eastern Desert (NED) of Egypt (Fig. 1). The region spreads between latitudes 28° 05'38" and 28° 27'40"N, and longitudes 32° 04'36" and 32° 40'22.76"E, incorporating an area around 2400 km². Different lithologic units differing in age from Precambrian to Quaternary represent the revealed rock assemblages in Samr El-Qaa region.

Samr El-qaa territory is divided by numerous wadies, which principally are structurally dominated and run towards the east. The study area is characterized by mountainous topography in its eastern portion which greatly occupied by hills of basement foundations (essentially composed of volcanics and granites). While, the western portion is filled with sedimentary deposits, which is less complex and mountainous than the eastern ones (Hassanein and Soliman, 2009).

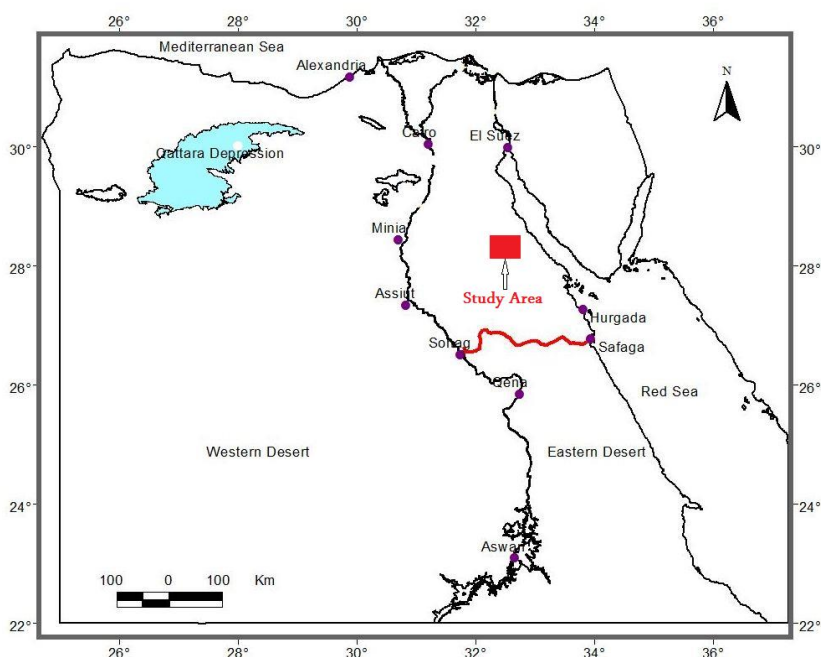


Figure 1: Map of Egypt explaining the area of Samr Elqaa in the NED.

The Eastern Desert (ED) of Egypt identified by three main basement zones i.e: north (NED), central (CED), and south (SED). CED is isolated from NED by a structure characterized by the NW dipping strike-slip fault (Stern and Hedge, 1985; Greiling et al., 1994). Stern and Hedge (1985), using radiogenic ages and field observations of the largest types of rock assemblages in the ED, concluded that the NED is defined by the recent rocks, while the oldest units are prevailing in the SED and CED. The present of Ediacaran non-metamorphosed volcano-sedimentary successions (590–630 Ma), including Dokhan Volcanics and Hammamat Sediments (Ressetar and Monard, 1983) is the essential characteristics of the NED (Breitkreuz et al., 2010).

However, Dokhan volcanic rocks are not always connected with Hammamat sediments, as the northernmost occurrences in the NED, such as Gabal Samr El-qa, are represented individually by Dokhan Volcanics and absence of the intercalations of Hammamat Sediments. Moreover, Plutons of Younger Granite and dykes are predominating in the NED, whereas there is a broad absence of ophiolites. Earlier volcanics (≈ 750 Ma) (Ali et al., 2009) occur greatly southward in the CED and SED and are divided into Younger and Older Metavolcanics, which are thought to be ophiolitic and island arc volcanics sequentially (Stern, 1981).

From most of the undeformed points and nonmetamorphosed of the volcanosedimentary series (i.e. Dokhan Volcanics and Hammamat Sediments), poverty shearing in Samr El-Qaa region of the NED can be revealed. Structural studies (e.g. Greiling et al., 1994; Fritz et al., 1996) illustrate a connected reduction of compression from the SED to the NED. The extra of compressional deformation can be observed as one of the main features in the SED and CED that are overprinted by transpression, while the extensional structures were the principal feature of the NED that was first overprinted by both reverse faulting and strike-slip notably to the north (Greiling et al., 1994).

Several lithologic assemblages, including diverse mixtures of sedimentary, igneous and metamorphic rocks are the foremost characters of Samr El-Qaa province. Furthermore, the position of the Suez Gulf at the eastern side of the study area in the NED gave the area additional significant frame. Accordingly, the area has been investigated by many authors [i.e. Bayoumi and Boctor (1970) and Ammar et al (2003)]. The geology of the study area is derived from map No. (NH36SW, Beni Suef, CONOCO, 1987). The geologic map of the study region (Fig. 2) describes that the area is coated by various varieties of the basement and sedimentary rock forms.

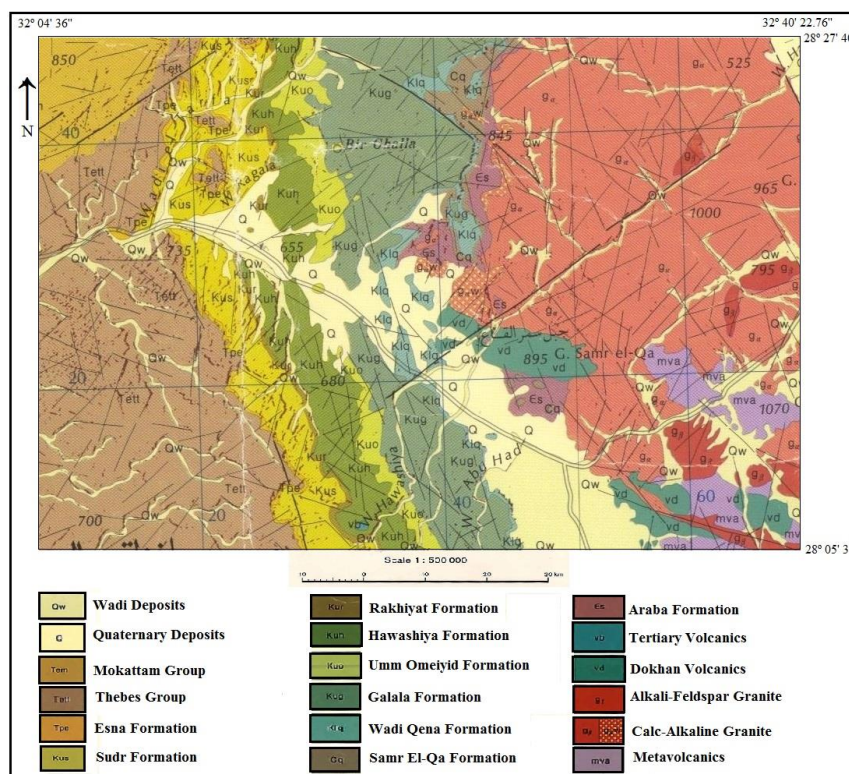


Figure 2. Geologic map of Samr El-Qaa area (After Conoco, 1987)

From the geologic map (Fig. 2) of the study region, it can be explained that the eastern part of the region is covered by basement rocks as Younger, Older, and metavolcanic rocks which are the principal associations of these basement units. Meantime, different deposits of sedimentary rocks occupy the western part of the study area varying in age from Paleozoic to Cenozoic. They include Shale of Samr El-Qaa and Esna Formations, Sandstones of Araba and Wadi Qena Formations, Limestone of Galala and Thebes Formations, Sudr Formation, Mokattam Formation, Hawashiya Formation, Umm Omeyid Formation, Rakhayat Formation, and Quaternary deposits. The junction zone between the basement and sedimentary rocks is interpreted as an unconformity contact (CONOCO, 1987).

3. AEROMAGNETIC DATA AND ENHANCEMENT TECHNIQUES

The reduced to the pole (RTP) magnetic data of Samr El-Qaa territory (Fig. 3) utilized in this research was obtained from the Egyptian Mineral Resources Authority collected by Western Geophysical Company of America in 1984, Aero Service section (1984). Aeromagnetic surveys were operated with a flight altitude of 120 m and the ordinary magnetic inclination was 39.5 N and declination was 2 E.

3.1. CET grid analysis:

CET grid method strengthens discontinuity zones within magnetic data and highlights essential irregularities in magnetic intensity. Structures are founded in the data by identifying multiple texture zones in the restricted magnetic response before the axes of symmetry examining. These axes are likely to detect straight abruption in the magnetic intensity. Frequently, areas of magnetic discontinuity are due to, and exhibit, rock edges, elongated structures, and intrusions which are important to assume the geologic framework of an area (Kovesi 1991).

Zones of magnetic discontinuity are expressed in the form of the skeletal structure by employing the texture enhancement. The output data describes each area of the discontinuity zones as skeletal line fragments that belong to each of them, visibly presenting the deviations in the directions and offsets within the structural characteristics (Kovesi 1997).

This technique employs the following actions:

- i. Texture Analysis Enhancement (Standard Deviation)– determines the regions of complicated textures connected with magnetic discontinuities.
- ii. Phase Symmetry – Utilizes the texture enhancement results for distinguishing zones of lateral discontinuity.
- iii. Detection of Structures – Uses the results of phase symmetry to reduce the discontinuities including zones into line-like structures.

Standard deviation affords a delineation of the local variation in the data. At each location in the grid, it measures the standard deviation of the data values within the local neighbourhood. Features of importance often present high variability with respect to the background signal. For a window containing N cells, whose mean value is μ , the standard deviation σ of the cell values x_i is given by:

$$\sigma = \sqrt{\frac{1}{N} \sum_{i=1}^N (x_i - \mu)^2} \quad (1)$$

When interpreting the results, values which approximate zero indicate very little variation, whereas high values indicate large variation.

3.2. CET porphyry analysis:

The CET Porphyry enhancement method (Holden E. J., et al., 2011) include:

- i. The Circular Feature Transform;
- ii. The Central Peak Detection;
- iii. The Amplitude Contrast Transform; and
- iv. The Boundary Tracing.

3.2.1. Circular Feature Transform:

The circular feature transform (CFT) adjusts an algorithm that computes the radial symmetry transform (Loy and Zelinsky, 2003), which is designed to distinguish circularly formed features. The transform highlights the centers of raised or depressed circular characteristics by recognizing where image gradients gather or conflict respectively. This plug-in allows the user to render parameters defining the radial size, circularity, and completeness of features of concern.

3.2.2. Central Peak Delineation:

The Central Peak Delineation step positions the centers of round features from a circular feature transform (CFT) output. This is accomplished by suppressing non-maximum circularity responses within each neighborhood in the data while

maintaining the maximum value. Thresholding is then implemented so that only important feature centers are retained. The outputs are a database file and a polygon file. The database file defines the circular feature centers, the radial symmetry strength, and the radius that produced in the greatest response (in both cells and meters). The polygon file includes, for each feature position, the circle boundary that produced the strongest radial symmetry response. This facilitates visualization of the size of the detected circular features (Holden E. J., et al., 2011).

3.2.3. Amplitude Contrast Transform:

The Amplitude Contrast Transform (ACT) method estimates the magnetic amplitude variance of circular features at particular distances from their surroundings to highlight the feature edges. A circular feature in the magnetic contrast transform output will appear as a 'halo', which corresponds to the circular edge of the feature (Holden E. J., et al., 2011).

4. RESULTS AND DISCUSSION

The RTP map (Fig. 3) of Samr El-Qaa area is distinguished by low magnetic intensity anomalies above the Quaternary deposits in the central and southern parts of the area. While the basement complexes in the eastern part show anomalies with moderate to high magnetic intensity. The large positive magnetic anomaly in the western part may reflect the presence of subsurface intrusions or indicate the thin cover of sedimentary deposits. RTP map shows that the most of magnetic anomalies are appeared to be structurally controlled along the NE, NNE, N-S and NW direction.

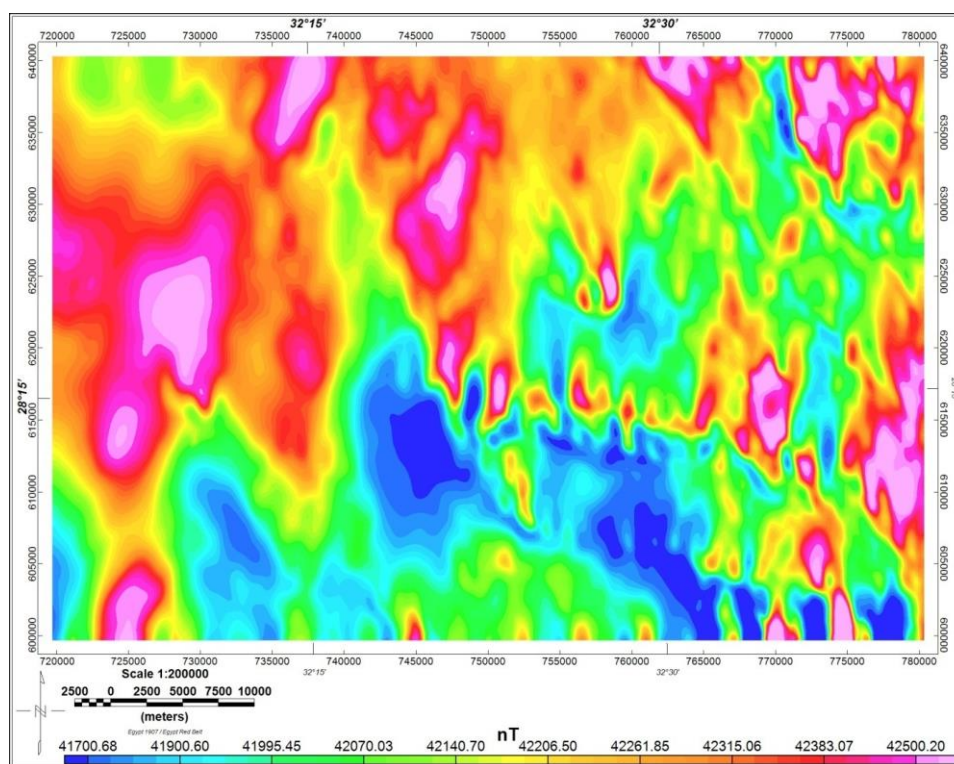


Figure 3. RTP map of Samr El-Qaa Area

4.1. Structural complexity detection:

The proceedings of the CET grid analysis are applied to the RTP map of Samr El-Qaa territory to produce in the structural complexity map.

Standard deviation map (Fig. 4) of the study shows that the low values which indicate very little variations are the main characteristics of the western part of the area that is associated with sedimentary rocks, whereas high values indicate large variations are associated with the basement rocks in the eastern part. The CET structural map (Fig. 5) that is derived from the standard deviation map of Samr El-Qaa territory shows that the eastern part is highly deformed and dissected by many tectonic trends. These trends are the N-S, NNE, NNW, NW, and NE directions.

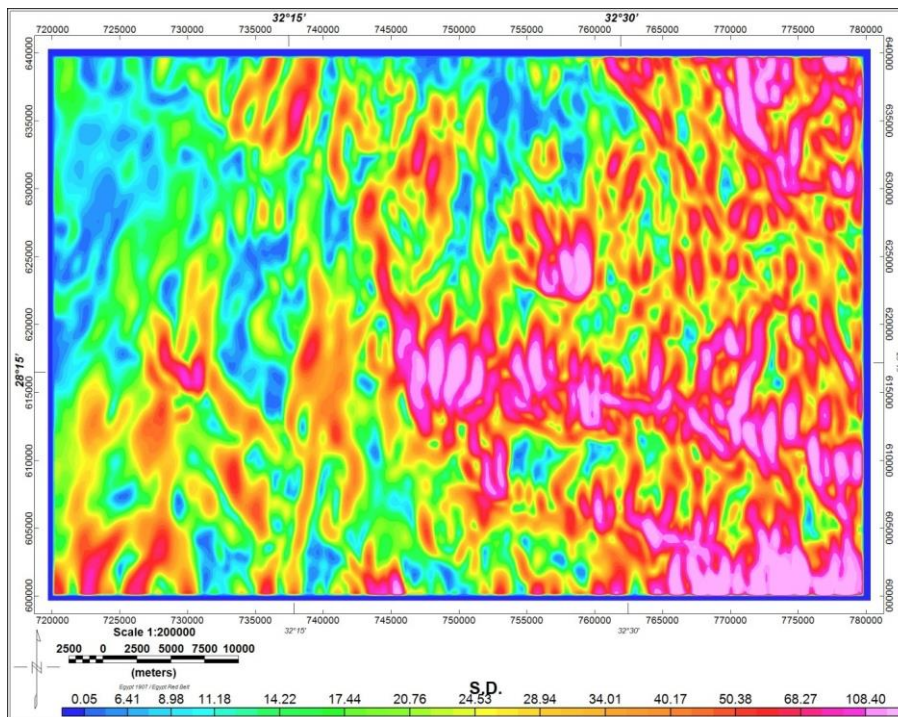


Figure 4. Standard deviation map of Samr El-Qaa area.

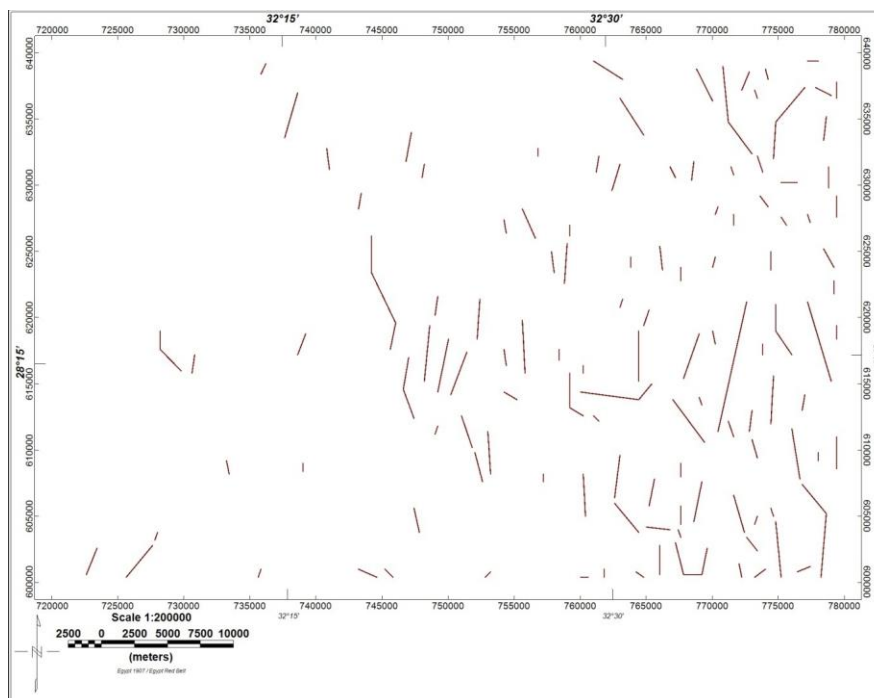


Figure 5. CET structural map of Samr El-Qaa area.

The structural complexity map (Fig. 6) overlain by the faults that are derived from Figure 5 classes the study area according to the deformity degree. Figure 6 shows that the eastern part associated with basement rocks of Samr El-Qaa territory is highly deformed along two main junction zones. The first one is observed in the southeastern corner trending in the N-S direction while the other one lies in the northeastern corner trending in the NE direction. Moreover, the structural complexity map (Fig. 6) illustrates that the central and southwestern parts are of intermediate structural complexity while the northwestern part is the lowest part of the study area from the complexity vision.

The structural complexity map (Fig. 6) can be used as a primary map for identifying the shear zones that can host mineralization in Samr El-Qaa region.

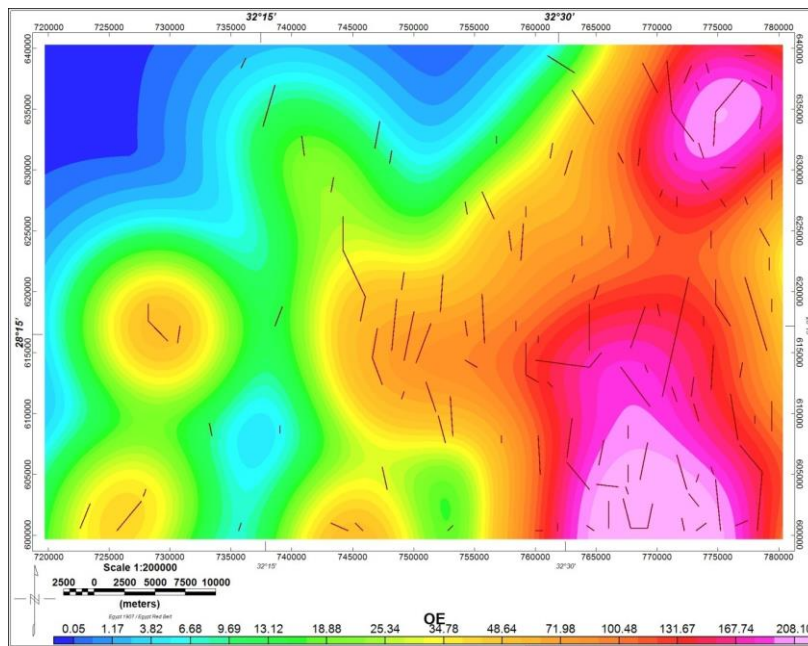


Figure 6. Structural complexity map of Samr El-Qaa area.

4.2. Detection of porphyry intrusions:

The steps of CET Porphyry analysis are applied to the red RTP map (Fig. 3) of Samr El-Qaa area to produce the CET porphyry map (Fig. 7). The CET porphyry map (Fig. 7) shows that the dike-like structures and porphyry structures in Samr El-Qaa area are associated with the multiple intersection zones that have been extracted from the CET structural map (Fig. 6) along the N-S, NNW, NNE, NW, and NE directions. The sedimentary deposits in the western part of Samr El-Qaa territory showed limited response to CET porphyry technique; while, the majority of resulted porphyry structures are associated with the basement complexes in the eastern part.

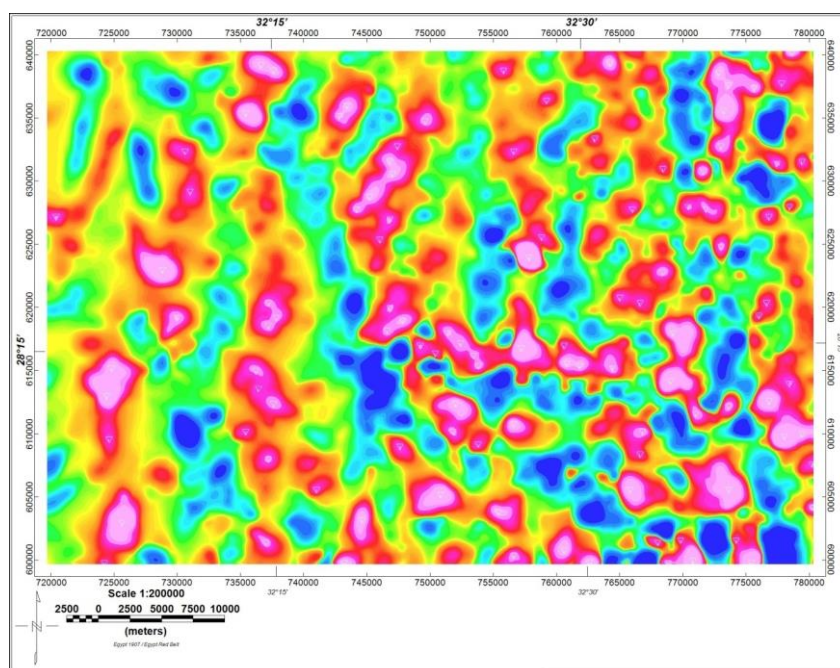


Figure 7. CET porphyry map of Samr El-Qaa area

5. CONCLUSIONS

The CET grid and porphyry analysis methods were applied to RTP map (TMI) of Samr El-Qaa area to detect the structural complexity zones and porphyry intrusions. The application of CET grid enhancement showed that the eastern part is highly deformed and dissected by many tectonic trends. These trends are the N-S, NNE, NNW, NW, and NE directions. Meanwhile, the utilization of CET porphyry method revealed that the dike-like structures and porphyry structures in Samr El-Qaa area are associated with the multiple intersection zones that have been extracted from the CET structural map.

As a general completion, it can be asserted that the application of CET grid and porphyry methods in Samr El-Qaa region successfully illustrated and mapped the zones of structural complexity and porphyry structures.

REFERENCES

- [1] Abdel-Rahman, M. A., and El-Etr, H. A., (1980): The orientational characteristics of the structural grain of the Eastern Desert of Egypt, In: El-Etr, H. A., Embabi, N. S. and Youssef, M. S. M., (ed.), *Geologic-Geomorphic Studies in the Egyptian Deserts*, Ain Shams Uni., Cairo, Egypt, (Abstract), 5 p.
- [2] Aero-Service (1984): Final Operational Report of airborne magnetic/ radiation survey in the Eastern Desert, Egypt, Conducted for the Egyptian General Petroleum Corporation, Aero- Service Division, Houston, Western Geophysical Co., Texas, USA.
- [3] Ali, K. A., Stem, R. J., Manton, W. I., Kimura, J. L., and Khamees, H. A., (2009): Geochemistry, Nd isotopes and U-Pb SHRIMP dating of Neoproterozoic volcanic rocks from the Central Eastern Desert of Egypt: new insights into the ≈ 750 Ma crust-forming event. *Precambrian Res.* 171, 1–22.
- [4] Ammar, A. A., Abdel-Rahman, M. A., Hassanein, H. I. E., and Soliman, K. S., (2003): Radiometric lithologic interpretation of aerial radiospectrometric false colour image maps, Eastern Desert, Egypt, *Arab Gulf Journal of Scientific researches*, 21(1): 28-47.
- [5] Bayoumi, A. I., and Boctor, J. G., (1970): Geological significance of gravity and magnetic anomalies in Rahmi area, Gulf of Suez district, U.A.R. 7th Arab Pet. Con., Secret. Gen. Leag. Arab State, Kuwait, Mar. 1970, 2(36): B-2, 28 p.
- [6] Breitkreuz, C., Eliwa, H., Khalaf, I., El Gameel, K., Bühler, B., Sergeev, S., Larionov, A., and Murata, M., (2010): Neoproterozoic SHRIMP U–Pb zircon ages of silica-rich Dokhan volcanics in the North Eastern Desert, Egypt. *Precambrian Res.* 182,163–174.
- [7] Core, D., Buckingham, A., and Belfield, S., (2009): Detailed structural analysis of magnetic data — done quickly and objectively. *SGEG Newsletter*. (April).
- [8] Conoco Coral (1987): Geological Map of Egypt, Scale 1: 500,000, -NH36SW- Beni Suef, Egypt. The Egyptian General Petroleum Corporation, Cairo (EGPC), Egypt.
- [9] Domzalski, W., (1966): Interpretation of aeromagnetic in evaluation of structural control of mineralization, *Geophysics Prosp.*, 14 (3): 273-291.
- [10] Eldosouky, A. M., Abdelkareem, M., and Elkhateeb, S.O., (2017): Integration of remote sensing and aeromagnetic data for mapping structural features and hydrothermal alteration zones in Wadi Allaqi area, South Eastern Desert of Egypt. *Journal of African Earth Sciences* 130 (2017) 28-37.
- [11] Eldosouky, A .M., and Elkhateeb, S. O., (2017): Texture analysis of aeromagnetic data for enhancing geologic features using co-occurrence matrices in Elallaqi area, South Eastern Desert of Egypt. *NRIAG Journal of Astronomy and Geophysics*, <https://doi.org/10.1016/j.nrjag.2017.12.006>.
- [12] El-Gaby, S., (1983): Architecture of the Egyptian basement complex, *Proceed. 5th Intern. Conf. Basement Tectonics*, Cairo, Egypt.

- [13] Fritz, H., Wallbrecher, E., Khudeir, A. A., Abu El Ela, F., and Dallmeyer, D. R., (1996): Formation of Neoproterozoic metamorphic core complexes during oblique con-vergence (Eastern Desert, Egypt). *J. Afr. Earth Sci.* 23, 311–329.
- [14] Gay, S. P. Jr., (1972): Fundamental characteristics of aeromagnetic lineaments, their geological significance, and their significance to geology. *The New Basement Tectonics* American Stereo map Company, Sult Lake City, Utah., 94p.
- [15] Greiling, R. O., Abdeen, M. M., Dardir, A. A., El Akhal, H., El Ramly, M. F., Kamal El Din, G. M., Osman, A. F., Rashwan, A. A., Rice, A. H. N., and Sadek, M. F., (1994): A structural synthesis of the Proterozoic Arabian-Nubian Shield in Egypt. *Geol. Rundsch.* 83,484–501.
- [16] Hassanein, H. I. E., and Soliman, K. S., (2009): Aeromagnetic Data Interpretation of Wadi Hawashiya Area for Identifying Surface and Subsurface Structures, North Eastern Desert, Egypt. *JKAU: Earth Sci.*, Vol. 20 No. 1, pp: 117-139.
- [17] Holden, E. J., Dentith, M., and Kovesi, P., (2008): Towards the Automatic Analysis of Regional Aeromagnetic Data to Identify Regions Prospective for Gold Deposits., *Computers & Geosciences*, Volume 34, Number 11, pp. 1505–1513.
- [18] Holden, E. J., Fu, S. C., Kovesi, P., Dentith, M., Bourne, B., Hope, M., (2011): Automatic identification of responses from porphyry intrusive systems within magnetic data using image analysis. *Journal of Applied Geophysics* 74 (2011) 255–262.
- [19] Kovesi, P., (1991): Image features from phase congruency, *Videre: Journal of Computer Vision Research*, Summer, Volume 1, Number 3, The MIT Press.
- [20] Kovesi, P., (1997): Symmetry and asymmetry from local phase, *AI'97, Tenth Australian Joint Conference on Artificial Intelligence*. 2 - 4.
- [21] Loy and Zelinsky, (2003): “Fast Radial Symmetry for Detecting Points of Interest”, *IEEE Transactions on Pattern Analysis and Machine Intelligence*, 25(8), 959–973.
- [22] Ressetar, R., and Monard, J. R., (1983): Chemical composition and tectonic setting of the Dokhan Volcanic formation, Eastern Desert, Egypt. *J. Afr. Earth Sci.* 1, 103–112.
- [23] Said, R., (1962): *The Geology of Egypt*, Elsevier Publ. Co., Amsterdam-New York, 337 p.
- [24] Sharma, P. V., (1997): *Environmental and Engineering Geophysics*, Cambridge University Press.
- [25] Stern, R. J., (1981): Petrogenesis and tectonic setting of late Precambrian enzymatic volcanic rocks, Central Eastern Desert of Egypt. *Precambrian Res.* 16, 195–230.
- [26] Stern, R. J., and Hedge, C. E., (1985): Geochronologic and isotopic constraints on Late Pre-cambrian crustal evolution in the Eastern Desert of Egypt. *Am. J. Sci.* 285, 97–127.
- [27] Williams, D. J., and Shah, M., (1990): A fast algorithm for active contours. *Proceedings of the Third International Conference on Computer Vision*, pp. 592–595.